

LETTER • OPEN ACCESS

Quantifying the climate response to extreme land cover changes in Europe with a regional model

To cite this article: Francesco Cherubini *et al* 2018 *Environ. Res. Lett.* **13** 074002

View the [article online](#) for updates and enhancements.

Related content

- [Biophysical effects on temperature and precipitation due to land cover change](#)
Lucia Perugini, Luca Caporaso, Sergio Marconi *et al.*
- [Impacts of land use and land cover change on regional climate: a case study in the agro-pastoral transitional zone of China](#)
Qian Cao, Deyong Yu, Matei Georgescu *et al.*
- [Adapting observationally based metrics of biogeophysical feedbacks from land cover/land use change to climate modeling](#)
Liang Chen and Paul A Dirmeyer

Recent citations

- [East Asian Summer Monsoon Representation in Re-Analysis Datasets](#)
Bo Huang *et al*

Environmental Research Letters



LETTER

Quantifying the climate response to extreme land cover changes in Europe with a regional model

OPEN ACCESS

RECEIVED

26 January 2018

REVISED

23 May 2018

ACCEPTED FOR PUBLICATION

24 May 2018



PUBLISHED

21 June 2018

Original content from this work may be used under the terms of the [Creative Commons Attribution 3.0 licence](https://creativecommons.org/licenses/by/3.0/).

Any further distribution of this work must maintain attribution to the author(s) and the title of the work, journal citation and DOI.



Francesco Cherubini^{1,3} , Bo Huang¹, Xiangping Hu¹, Merja H Tölle²  and Anders Hammer Strømman¹

¹ Industrial Ecology Programme, Department of Energy and Process Engineering, Norwegian University of Science and Technology (NTNU), Trondheim, Norway

² Department of Geography, Climatology, Climate Dynamics and Climate Change, Justus-Liebig University Giessen, Giessen, Germany

³ Author to whom any correspondence should be addressed.

E-mail: francesco.cherubini@ntnu.no

Keywords: regional climate, land cover change, biophysical mechanisms

Supplementary material for this article is available [online](#)

Abstract

Many future scenarios expect a key role for the land use sector to stabilize temperature rise to 2 °C or less. Changes in land cover can influence the climate system, and the extent and magnitude of the anthropogenic modifications at local and regional scales is still largely unexplored. In this study, we use the regional climate model COSMO-CLM v.4.8 to quantify the climate response to idealized extreme land cover changes in Europe. We simulate four idealized land use transitions involving abrupt conversion of today forestland to bare land or herbaceous vegetation, and conversion of today cropland to evergreen needle-leaf forest or deciduous broad-leaf forest. We find that deforestation to bare land and herbaceous vegetation causes an annual mean regional cooling of -0.06 ± 0.09 (mean \pm standard deviation) and -0.13 ± 0.08 , respectively. Afforestation to needle-leaf and broad-leaf forests leads to a mean warming of 0.15 ± 0.09 °C and 0.13 ± 0.09 °C, respectively. Precipitation declines after forest clearance and increases with afforestation, but the spatial variability is high. Temperature impacts are usually more significant in the grid cells affected by land cover change and show a clear latitudinal pattern and seasonal variability. The mean temperature response to deforestation turns from positive to negative between 50 and 55° latitude, and shows the strongest cooling in spring (>2 °C, high latitudes) but warming in summer (>1 °C), when the average number of hot days is increased. Afforestation has the major average warming impacts in winter, where the frequency of cold temperature extremes is reduced. Overall, biophysical effects from land cover changes shape European climate in different ways, and further developments can ultimately assist decision makers to modulate land management strategies at different scales in light of climate change mitigation and adaptation.

1. Introduction

Land management plays a key role in future strategies for climate change mitigation. Many future scenarios envision extensive land use transitions, especially under stringent temperature targets [1–5]. In the different Shared Socio-economic Pathways, global forest areas are predicted to change from about –500 Mha up to +1000 Mha in 2100, and between 200 and 1500 million ha of land will be required to grow bioenergy crops [2]. The higher-end of this range is achieved

under the most ambitious climate change mitigation targets.

A change in land cover has impacts on climate through modification of the surface energy and water budget, mediated by changes in biophysical effects like surface albedo, evapotranspiration, and surface roughness [6, 7]. The net effect on local climate is a balance of these mechanisms, and it is highly spatially heterogeneous. The partitioning of available energy into latent and sensible heat fluxes is sensitive to vegetation characteristics [8], and has a direct influence on local near-surface air temperature and water availability

[9–11]. A global latitudinal pattern in the net balance of biophysical effects has been detected by both modelling [12–16] and observational studies [17–21]. In the tropics, evapotranspiration effects dominate and reinforce the climate benefits of CO₂ sequestration in trees at a regional and global scale. At higher latitudes, the contribution from surface albedo is stronger, especially in areas affected by seasonal snow cover, and counteracts the carbon benefits. At mid-latitude, there are major uncertainties and spatial variability in the climate response, especially at a local scale [6, 9, 22].

Climate change impacts tend to be underestimated at a regional level, because the projected global mean temperature changes are dampened by averaging over the oceans, and are much smaller than the expected regional effects over most land areas [23–25]. This applies to both mean and extreme effects [26], as changes in regional extremes can be greater than those in global mean temperature up to a factor of three [23]. Long-term studies show that land use and land cover changes have little influence on the atmospheric circulation compared to greenhouse gas forcing [27–29], but land-atmosphere processes can affect and modify temperature and precipitation variability [30, 31], including extremes [22, 32]. Previous model-based studies of land-climate interactions are contrasting, especially at mid-latitudes. Review studies of land use change and regional climate find significant spatial heterogeneities, and results do not allow to derive conclusions that hold at different locations and across scales [6, 7, 9]. Some studies show that deforestation reduces near surface air temperature, daily temperature extremes, and the number of summer hot days [33–35], while others find increases in the occurrence of hot-dry summers [22, 36, 37].

There is thus a need for extensive quantification and better understanding of biophysical land-climate interactions and their effects on regional climate [9, 38–40]. The EURO-CORDEX & LUCID initiative recently launched the inter-model comparison LUCAS ('Land Use and Climate Across Scales') with the aim to assess biophysical impacts from land use changes in Europe [41]. The inclusion in future climate policy contexts of regional temperature and precipitation effects of land cover changes can maximize possible synergies of climate mitigation and adaptation policies, from the local to the global scale [9, 23]. To the best of our knowledge, no previous analyses applied a regional climate model across the entire European CORDEX domain to study the effects of extreme land cover changes on regional climate. In this work, we perform a series of experiments to test the sensitivity of the regional climate model COSMO-CLM to idealized land cover changes in Europe in terms of near-surface air temperature, precipitation, and temperature extremes. Although we acknowledge the limitations of a single model output relative to multi-model means, this analysis provides extensive quantitative findings and it is a step towards increasing

the availability of information regarding the biophysical climate response to land cover changes in Europe.

2. Methodology

2.1. Model description

The regional climate model COSMO-CLM (CCLM) version 4.8 is applied in this study [42]. It is the climate version of the weather prediction model Consortium of Small-scale Modelling (COSMO) [43]. CCLM is found to be one of the best performing regional climate models of the EURO-CORDEX project with respect to temperature, precipitation, and surface fluxes assessed against observations across the European domain [40]. CCLM is a non-hydrostatic limited-area atmospheric prediction model that relies on the primitive thermodynamical equations describing compressible flow in a moist atmosphere. The model applies a split-explicit third-order Runge-Kutta time discretization [44] on an Arakawa-C horizontal grid [45]. The terrain follows height co-ordinate in the vertical level with rotated geographical co-ordinates [46]. The parameterization of precipitation is based on a four-category one-moment cloud-ice scheme that includes cloud, rainwater, snow, and ice. The physical parameterizations include a radiative transfer scheme [47], a cloud-microphysics parameterization, and a turbulent kinetic energy-based surface transfer.

To implement biophysical exchanges between the land surface, atmosphere, and soil, CCLM uses the soil-vegetation-atmosphere model TERRA-ML [48, 49]. TERRA-ML provides the lower boundary conditions for the atmospheric circulation model and gives information about surface and soil conditions by simultaneously solving the thermal and hydrological budgets. It uses a stability and roughness length-dependent surface flux formulation to model the turbulent exchange between the atmosphere and the underlying surface. The upper boundary condition is obtained by computing the energy balance at the surface. The hydrological part of TERRA-ML predicts soil water content by solving the Richards' Equation and estimates the water content of above-ground reservoirs such as snow and interception [50]. The source of water from the atmosphere is through precipitation, dew (on both plants and soils) and rime, and the sink terms are runoff and evapotranspiration. The soil module has 10 soil layers defined down to a depth of 15 m. The variables of the hydrological cycle are calculated using the multi-soil layer concept with soil moisture diffusion, and soil heat conduction equations are used for different soil textures as well as frozen soil processes. Plant transpiration and soil evaporation are parameterized using the Biosphere-Atmosphere Transfer Scheme. Net evapotranspiration is the sum of bare soil evaporation, plant transpiration, sublimation from the snow and evaporation from the interception storage, weighted by their respective areal

coverages. Hydrological processes are described in details elsewhere [49, 51].

The roughness length over land depends on the sub-grid scale variance of orography and land-use. The model takes the dominant vegetation type and soil texture for each grid cell, which is characterized by vegetation parameters such as leaf area index (LAI), plant coverage, root depth, and roughness length (z_0), which are defined for each land cover class. For LAI and plant cover, the model derives an annual cycle between minimum and maximum values using a growing and resting period according to latitude and a height correction factor [49]. Thus, phenology is influenced by seasonal variations, but there is not inter-annual variability. Forest areas are described in terms of fractions of the grid covered by deciduous or evergreen forest, and the major effects they exert in the model are through influence on snow albedo, surface roughness, and transpiration rate.

2.2. Simulations of land cover changes

Following the EURO-CORDEX framework, we set-up the simulations using the initial and lateral boundary conditions from the European Centre for Medium-Range Weather Forecasts Interim reanalysis [ERA-Interim; 52]. ERA-Interim data are selected for a larger area in order to clear the noise in the lateral boundary conditions for the external part of the domain. All simulations are performed using the EURO-CORDEX configuration for CCLM, which was developed after validation of the spatiotemporal patterns of the European climate against an observational reference [53]. We consider the period 1980–2010 at a horizontal resolution of 0.44 degrees with 40 atmospheric levels. We use a time step of 300 seconds, one year of model spin up time, and the Tiedtke mass-flux convection scheme for physical parameterization [54]. The control simulation (CTRL) is based on present-day vegetation cover and soil from the global land cover database GLC2000 [55].

Changes in land cover are simulated following the approach used in previous similar studies [26, 56]. In the deforestation experiments, grid cells where forest areas are dominant are converted to bare land (FOR to BL) or herbaceous vegetation (FOR to HV). In the afforestation experiments, grid cells where cropland are dominant are converted to evergreen needle-leaf forest (CROP to ENF) or to deciduous broad-leaf forest (CROP to DBF). In the changed grids, the land surface parameters are modified according to the new type of land cover and kept constant throughout the simulation period to maximize model response. Changes in plant biomass are represented by a modified roughness length, root depth, LAI, and vegetation coverage [26]. These structural changes in vegetation alter the surface and energy balance of the land surface. For example, while LAI influences the amount of intercepted water and the partitioning of energy fluxes into sensible and latent heat, the roughness length affects the turbulent

mixing of heat in the atmosphere, and the rooting depth determines the amount of water extracted from the soils by vegetation.

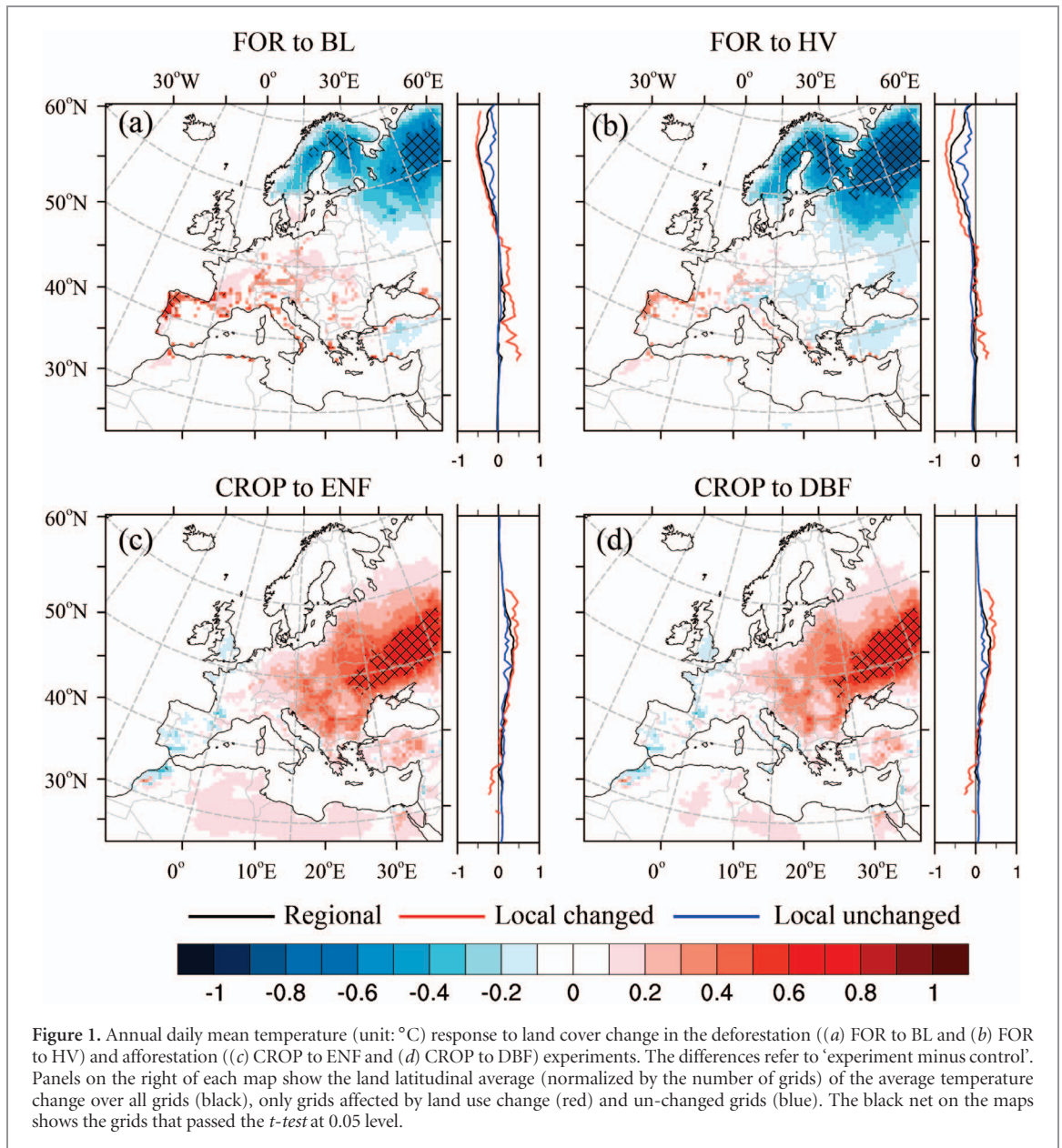
The most affected areas by the land cover transitions are the northern and eastern part of the domain in the deforestation experiments (1527 changed grids) and the central band of Europe crossing the domain from east to west in the afforestation experiments (1835 changed grids). See supplementary figure S1 available at stacks.iop.org/ERL/13/074002/mmedia for the spatial distribution of the grids. The impacts on regional climate are then computed by the difference between the respective experiment and the control run.

These idealized land use conversions are designed to study model's response to potential maximum land modifications. Since lateral boundary conditions do not vary between experiments and control run, the resulting differences can be attributed to the simulated land cover changes and illustrate the interactions between the land surface characteristics represented in COSMO-CLM and climate at regional scales [26]. Results are investigated in terms of temperature and precipitation response over land, for both the entire domain (regional) and affected grids only (local), their spatial, seasonal and diurnal variability, and frequency of temperature extremes. The latter is estimated using the tails (5th and 95th percentile) of the temperature probability density function for each grid of the domain [57, 58]. We then count the average number of days per year in the different simulations of maximum average daily temperature above the 95th percentile (hot extremes), or minimum average daily temperature below the 5th percentile (cold extremes), relative to the control run.

3. Results and discussion

3.1. Temperature response to deforestation

Figure 1 shows the spatial distribution of the mean temperature response in Europe to the four extreme land cover changes. The annual mean regional cooling is -0.06 ± 0.09 °C (mean \pm one standard deviation) for FOR to BL and -0.13 ± 0.08 °C for FOR to HV. Impacts are stronger at a local scale on the grids affected by the land cover change. There is a significant spatial gradient in the average temperature response to deforestation, with an average cooling in the northern and eastern part of the domain, and a warming effect in western and central Europe. The replacement of forests with bare land or herbaceous vegetation increases surface albedo and reduces absorbed radiation, especially during winter months in areas affected by seasonal snow cover owing to the well-known snow effect on surface albedo [59, 60]. In some northern locations, the decreased absorption of solar radiation at the surface results in annual mean cooling that can achieve annual mean values around -1 °C. On the other hand, in central and southern Europe, the relative importance



of turbulent fluxes increases and the net effect is a warming contribution that can be up to 0.8 °C for BL and 0.6 °C for HV (figures 1(a) and (b)). In these cases, changes in evapotranspiration fluxes and surface roughness dominate. Bare land and herbaceous vegetation have a different partitioning between sensible heat and latent heat than forestland. Forests have a larger latent heat flux (up to 15 W m⁻²) and smaller sensible heat flux (up to 10 W m⁻²), especially during summer months (see supplementary figure S2 and S3 for details on latent and sensible heat fluxes). The transition to HV generally tends to have a more cooling effect than to bare land. The reason is that bare land does not have vegetation, and has a higher energy partitioning to sensible heat than HV, which on the other hand has larger latent heat fluxes that contribute to a cooler surface.

A clear latitudinal pattern emerges from the results. At increasing latitude, the average temperature response to deforestation declines and turns to

negative (i.e. cooling) from about 50°–55° N. The net impact of changes in biophysical factors on climate strongly depends on local climate and vegetation type, especially at mid-latitude areas where the opposing albedo and evapotranspiration effects are of comparable size but different sign. Depending on the location, the dominant effect can be an average annual warming or cooling, as shown by the heterogeneities of the responses in figure 1. The situation differs at high latitude, where the temperature response is clearly negative (cooling). Such a latitudinal pattern of temperature response to land cover changes is reported by other modelling and observational studies. The latitudinal threshold is found to be around 30° N (global average) using a fully coupled global circulation model [12], and the use of an earth system model of intermediate complexity achieves similar conclusions [16]. Empirical studies identify the transition from warming to cooling at higher latitudes. Using a semi-empirical

approach, annual mean temperature response to deforestation is found to turn to negative values around 60° N at a global level, but at appreciably lower latitudes (around 50° N) in Europe [21]. In another global site-pair analysis, the transition is found at about 50° N (global average) [18]. Using data from weather stations, the transitional latitude is found to occur between 35 and 45° N in America and eastern Asia [19, 20].

Other modelling studies, mostly based on global models, reported an average regional cooling from deforestation to grassland of -1.96 ± 1.44 °C in boreal climates, and of -0.73 ± 0.45 in temperate climates [9]. Our findings generally fall in the lower end of the range for boreal deforestation and are outside the range for mid-latitudes, for which we do not estimate a significant cooling effect. Our outcomes of -0.41 ± 0.25 and -0.04 ± 0.09 of regional temperature changes in FOR to HV for boreal and temperate climates are rather closer to the ranges reported from observation-based studies, i.e. -0.59 ± 0.54 °C and $+0.50$ ($-0.21/1.2$) °C, respectively [9]. To facilitate comparison with past and future studies, we report averages of temperature and precipitation differences for boreal and temperate climates from our analysis in supplementary table S1.

3.2. Temperature response to afforestation

Afforestation generally causes a warming effect in large areas of Europe (figures 1(c) and (d)). The annual mean regional warming is 0.15 ± 0.09 °C for CROP to ENF and 0.13 ± 0.09 °C for CROP to DBF. As in the deforestation case, impacts are stronger at a local scale on the grids affected by the land cover change (up to about 0.9 °C in some locations). The magnitude and significance of the warming gradually increases at high latitudes and in the eastern part of the domain, and the variability in the response is the highest at mid-latitudes. The lower albedo values of forestland over cropland increases the net radiation at the surface, thereby causing a net warming effect. Relative to the CTRL run, tree cover generally reduces surface albedo, thereby increasing both net radiation at the surface and latent and sensible heat fluxes. DBF has higher latent heat fluxes and lower sensible heat fluxes than ENF because of the higher water transpirations of leaves and larger LAI. ENF also has lower latent heat fluxes than CROP in summer (supplementary figure S2). Other studies found a net warming effect of tree cover at mid and high latitude [12, 14–16, 28], although the trend is not so clear in semi-empirical studies [19, 21].

The warming effect of afforestation increases at higher latitudes, and, to some extent, a longitudinal gradient can also be appreciated. In both afforestation experiments, areas towards the western part of Europe show a slight cooling effect, whereas the warming effect becomes increasingly dominating while moving towards the eastern part of the domain. A transition from cooling to warming occurs between 0 and 10° E longitude. A similar pattern, but of opposite sign, can

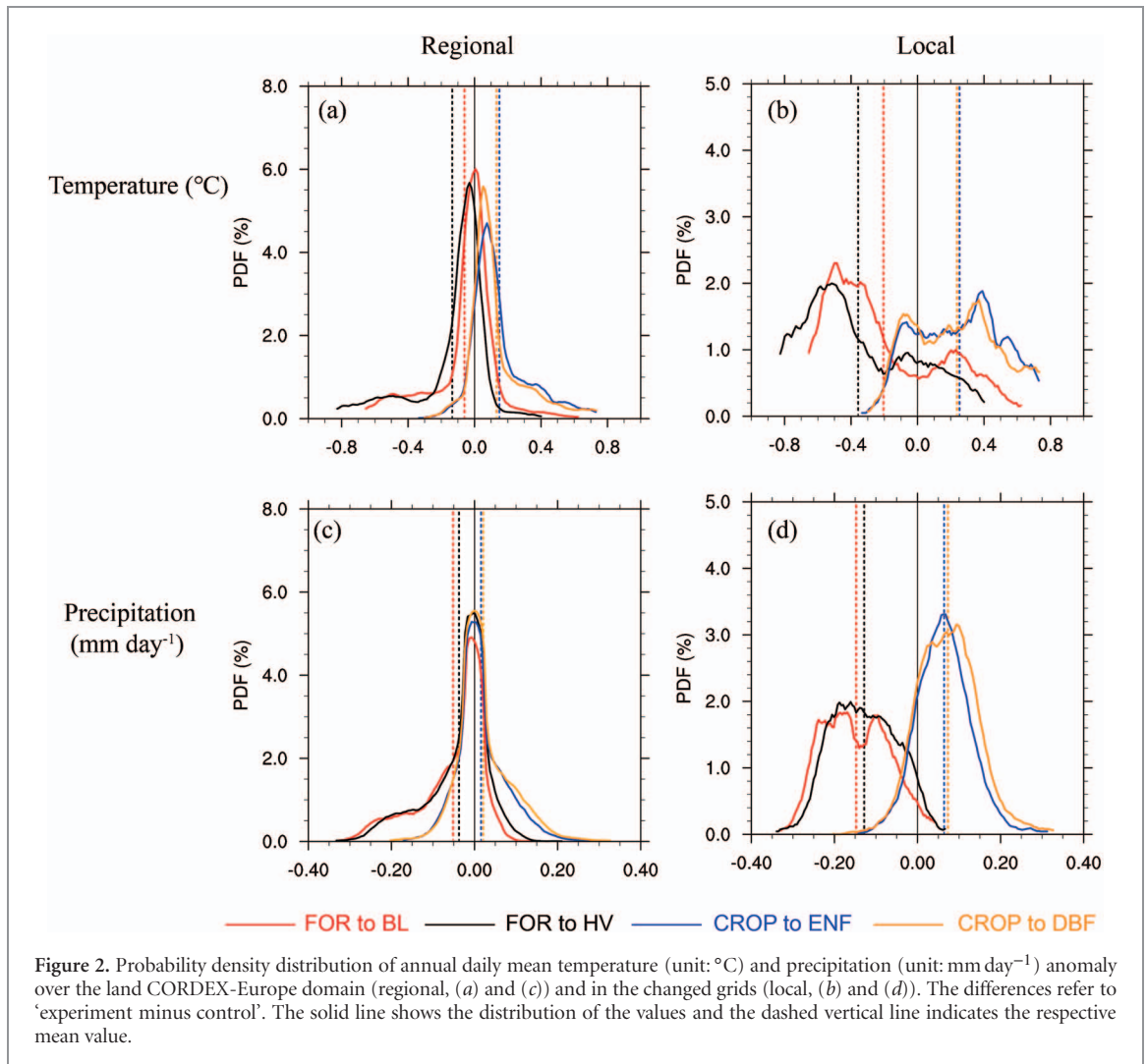
be appreciated in the deforestation to HV, whereas the change in temperature sign occurs at higher longitudes (about 30° E) for BL in temperate climates. This trend is difficult to interpret. Empirical studies show that forests have the tendency to decrease surface temperature compared to cropland in relative proximity to oceans, mainly through larger surface evaporation and greater roughness length [18, 20]. These mechanisms are confirmed by recent remote sensing-based estimates [21, 61], and our findings generally align with other modelling experiments [16]. The latter concludes that temperature changes largely result from the specific climate conditions in which the land use change occurs and is less influenced by the magnitude of individual biophysical changes.

3.3. Precipitation response

The precipitation response to the simulated extreme land cover changes has large spatial variability (see supplementary figure S4). In the deforestation experiments, a significant dryer climate is found over the EURO-CORDEX domain, especially over the affected grids. The annual mean difference across the entire domain is -0.05 ± 0.02 mm day⁻¹ for FOR to BL, and -0.04 ± 0.02 mm day⁻¹ for FOR to HV. Local responses can be up to -0.4 mm day⁻¹. Removal of trees causes a significant reduction in regional precipitation owing to reduced evapotranspiration, which is stronger in the transition to bare land than herbaceous vegetation. On the other hand, afforestation generally increases precipitation in major places of central and northern Europe, although changes are generally not significant and do not pass the *t-test* (0.05 level) in most of the grids. The average change across the domain is 0.02 ± 0.02 mm day⁻¹ for both CROP to ENF and CROP to DBF experiments. It is generally difficult to detect the signal of vegetation cover changes on precipitation owing to the inherent variable frequency of rainfall patterns, and the presence/absence of vegetation is usually more important than the vegetation type [9]. At high latitude, evapotranspiration is constrained by net radiation, while at lower latitudes the supply of water becomes the limiting factor and spatial heterogeneities increase [62]. This can explain the more significant response observed in the deforestation experiments, as forests are largely placed in northern Europe.

3.4. Local and regional climate signals

The climate change signal for the different experiments over the entire domain and the grids affected by the change in land cover is summarized in figure 2 as a probability function based on kernel density estimation. The distribution of the climate signal is more spread at a local scale (figures 2(b) and (d)) than at a regional scale (figures 2(a) and (c)). In the deforestation experiments, the probability distribution of local temperature changes peak at around -0.5 °C (up to more than 2% of total grids), with the FOR to HV

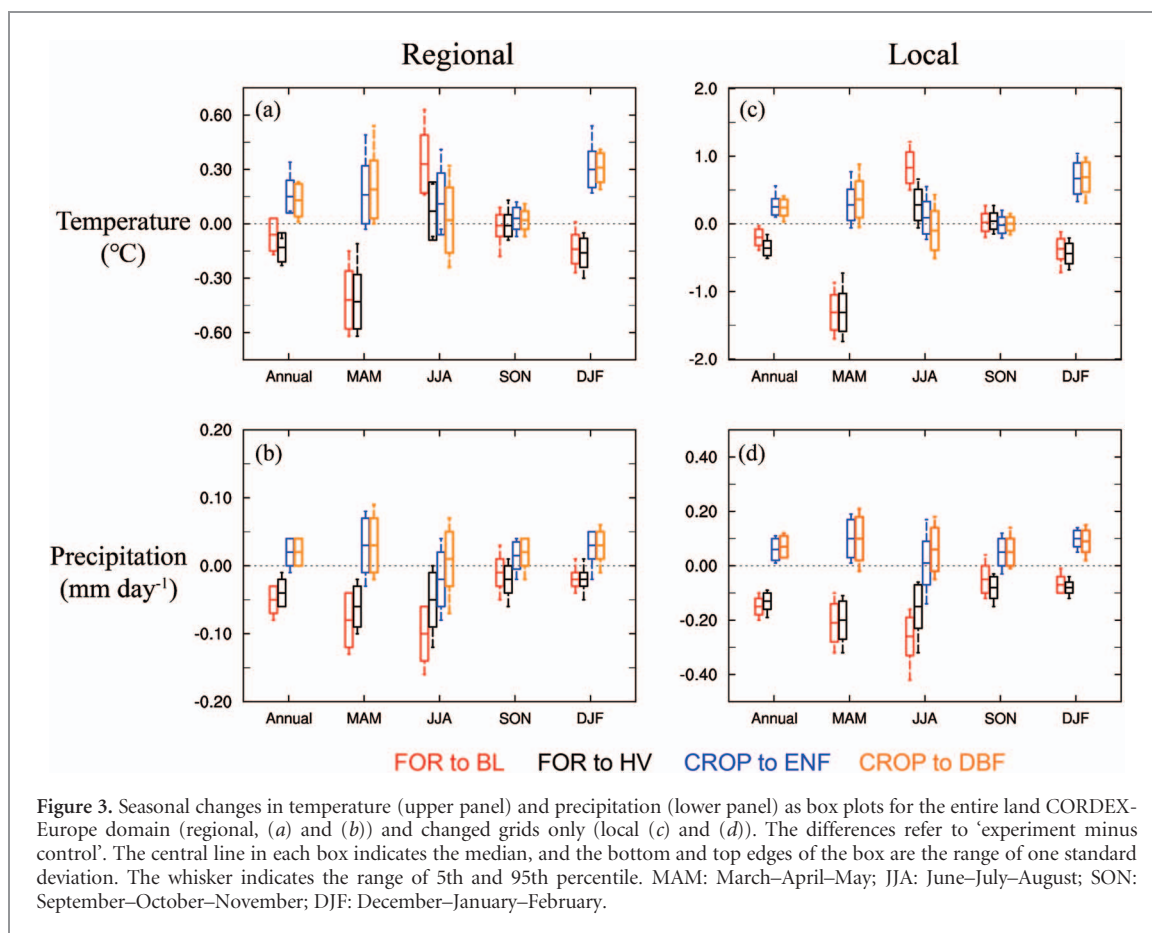


case exhibiting a distribution (and average estimate) more translated towards higher temperature reductions (figure 2(b)). Afforestation experiments show two similar peaks in local temperature changes, one around -0.1 °C (for about 1.5% of the sample) and the other around $+0.5$ °C (for about 2% of the sample). Precipitation changes are rather similar and follow a bell-like shape curve around the mean estimate. Differences in the climate signal from the two afforestation experiments are relatively small, and the probability distributions follow a similar pattern for both temperature and precipitation changes.

3.5. Seasonality and diurnal cycle

Temperature impacts from deforestation show a cooling effect in winter and spring, but warming in summer and little differences in autumn (figure 3; see supplementary figure S5 for a spatial distribution of the seasonal temperature differences). The largest cooling occurs in spring, where average temperature changes are about -0.42 ± 0.16 °C at a regional level, and -1.31 ± 0.26 °C when impacts are averaged on local affected areas, where the cooling can be up to -1.8 °C (5th percentile). This strong cooling in spring is largely due to the combination of larger solar radiation with

high differences in surface albedo, which drives a significant reduction in the net radiation balance. A couple of considerations supports this insight. First, there are no major differences between BL and HV in spring, meaning that the vegetation control on temperature changes is minimal, suggesting that climatic conditions act as the main driver. Second, the diurnal temperature cycle in spring shows the maximum cooling around mid-day, under the highest radiation load (figure 4(b)). The larger radiation flux in spring can also explain the stronger cooling observed in spring than winter. Temperature impacts significantly turn to positive in summer. At a local level, temperature increases up to 0.83 ± 0.23 °C for BL, and 0.28 ± 0.23 for HV (figure 3(c)). In summer, the incoming radiation is at a maximum but differences in surface reflectivity are small, meaning that reductions in evapotranspiration and surface roughness are the main drivers for such a warming effect. The difference between BL and HV underlines the importance of vegetation to keep a cooler climate in summer. BL has smaller values of latent heat fluxes than HV all year round, but especially during summer months, where fluxes of sensible heat are in turn larger (supplementary figures S6 and S7). The diurnal temperature cycle in summer has



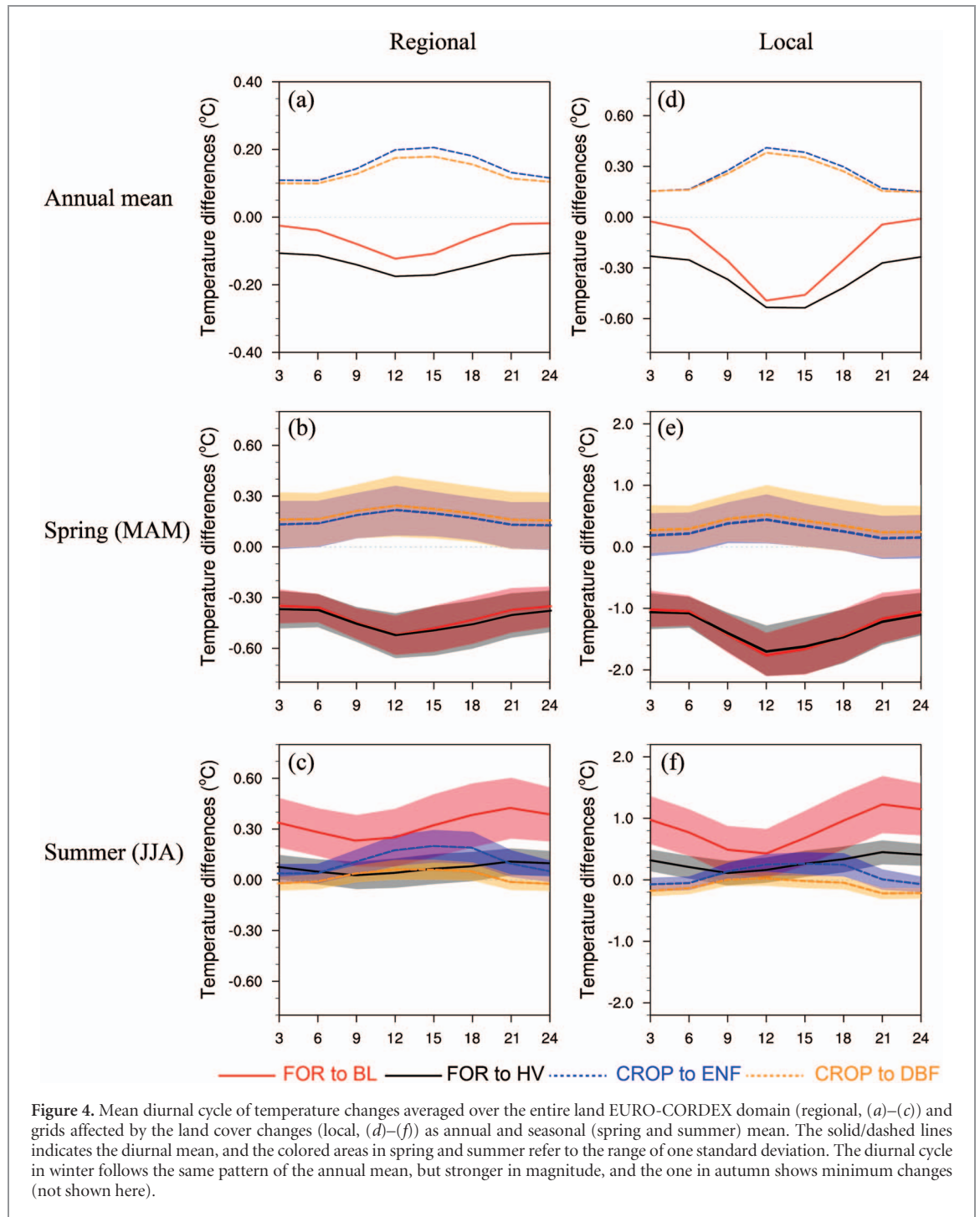
a different pattern with respect to the annual mean (figure 4(c)). Both BL and HV have higher temperature differences at night, driven by higher sensible heat fluxes that peak between 6 and 9 p.m. in summer (see supplementary figure S8).

Afforestation experiments show a temperature change that has lower variations over the year. The maximum warming is achieved in winter, followed by spring (figures 3(a) and (c)). This is opposed to deforestation experiments, where the temperature response is stronger in spring than winter. This can be connected to the average warmer conditions achieved after afforestation, which anticipates snow melting and reduces snow cover in spring. Temperature changes are highly variable in summer and autumn, for which the average sign of the impact is not clear. Temperature changes in summer are generally higher for ENF than DBF, mostly due to the lower latent heat fluxes of coniferous forests than cropland or deciduous forests. For DBF, average impacts in summer are a cooling effect (-0.10 ± 0.29 °C), although spatial variability is high (supplementary figure S5) and at local scales temperature changes can achieve up to about ± 0.5 °C (5th and 95th percentile). Over the diurnal cycle, ENF has a relatively higher average temperature impact than DBF in summer days, with temperatures that are slightly cooling at night (figure 4(f)). This difference is due to the different evapotranspiration efficiencies of the trees.

Precipitation changes usually have a more average consistent pattern across the seasons, although the spatial variability is large (figures 3(b) and (d)). Deforestation tends to reduce the transfer of water vapor from the soil to the atmosphere, and therefore it decreases average precipitation. Conversion to HV has smaller effects on rainfall than BL because the presence of vegetation reduces the evapotranspiration gradient with previous forest cover. This is indicated by higher levels of soil water content in BL than HV and relative to control run in the deforestation experiments (supplementary figure S9). Afforestation experiments tend to increase rainfall, especially in spring, and in presence of DBF. The needles in ENF constraint evapotranspiration, mainly during summer months, and soil water content levels exhibit the strongest increase for this land transition. This may have consequences for future climate in mid-latitudes as projected climate changes indicate wetter winters and consequently a delayed soil drying in spring and early summer [63].

3.6. Temperature extremes and correlation analysis

Occurrence of temperature extremes are summarized in table 1, where the average difference in number of hot/cold days is shown per season and at a regional or local scale (see figure S10 for their spatial distribution). Deforestation increases the number of hot days in summer, up to about 15 days for BL and more



than 4 days for HV (local scale). However, variability is large, especially for HV, where the number of hot days actually declines in many locations (no clear latitudinal or longitudinal pattern emerges). In general, a dual effect of evaporation contributes to increase hot temperature extremes. Deforestation reduces evapotranspiration rates and this effect is dominant in summer, with warmer surface. The decrease in evapotranspiration also decreases cloud cover (supplementary figures S11 and S12), which results in an increase of absorbed radiation at the surface. This effect is amplified for the hot tail of the distribution in summer because of a decrease in cloud cover and associated

increase in the amount of absorbed solar radiation at the surface under high radiation loads. In winter and spring, the presence of cold days tend to increase at similar rates for BL and HV, but spatial variability is still large. These findings align with the studies that find a significant increase in summer hot days after deforestation [37].

Afforestation has an average warming effect in winter, where the occurrence of cold days is reduced (−3.61 and −3.70 days at a local level for ENF and DBF, respectively) and the number of hot days increases (4.46 and 5.54). This trend is generally consistent across the entire domain, for both ENF and DBF.

Table 1. Changes in occurrence of hot and cold temperature extremes, measured as average number of days (n) per season, in the different experiments at a regional and local scale. T_{max} refers to the average number of days in which the maximum average daily temperature is above the 95th percentile of the control run (hot temperature extremes). T_{min} refers to the average number of days in which the minimum average daily temperature is below the 5th percentile of the control run (cold temperature extremes). Results are left blank when $-1 < n < 1$.

Season	FOR to BL	FOR to HV	CROP to ENF	CROP to DBF	Legend (n = number of days)	
<i>Regional</i>						
T_{max}	Winter (DJF)		1.59	2.17	$n > 4$	
	Spring (MAM)				$2 < n < 4$	
	Summer (JJA)	6.72	1.2	3.74	1.22	$1 < n < 2$
	Autumn (SON)					$-1 < n < 1$
T_{min}	Winter (DJF)	1.68	2.59	-2.22	-2.33	$-2 < n < -1$
	Spring (MAM)	2.09	2.56	-1.93	-2.11	$-4 < n < -2$
	Summer (JJA)					
	Autumn (SON)			-1.39	-1.28	$n < -4$
<i>Local</i>						
T_{max}	Winter (DJF)	-1.49	-1.62	4.46	5.54	
	Spring (MAM)	-1.73	-1.71			
	Summer (JJA)	14.9	4.4	4.63		
	Autumn (SON)		1.73			
T_{min}	Winter (DJF)	4.37	5.87	-3.61	-3.7	
	Spring (MAM)	6.26	6.71	-3.17	-3.31	
	Summer (JJA)	-1.34				
	Autumn (SON)			-1.99	-1.73	

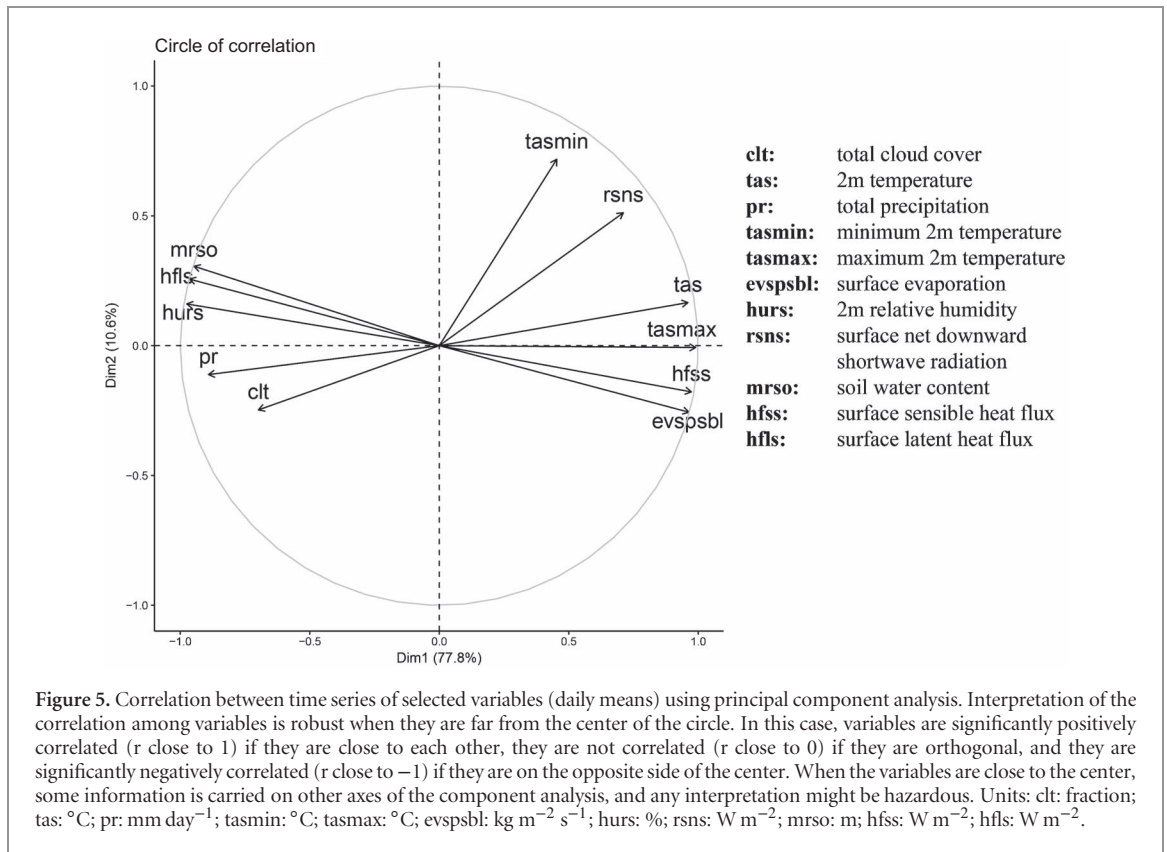
Spatial variability again becomes relevant in summer. For ENF, the lower evapotranspiration rate of needle-leaf trees increases the number of hot days relative to cropland in many grids of the domain. The smallest average change in summer hot days is observed for DBF (0.22 at a local level), which is the balance of a high spatial variability without a clear latitudinal or longitudinal pattern (figure S10). In some areas, like northern Germany and France, the presence of DBF mitigates the number of hot days in summer, in line with findings from previous studies [56], but in the western part of the Mediterranean basin the number of hot days can increase. Relative to ENF, DBF also shows a stronger reduction in the number of hot days in eastern Europe.

Most of the relationships among temperature and precipitation changes and physical processes discussed above are evident from the correlation circle shown in figure 5, which is based on the principal component analysis. The results show that almost 90% of the information (variance) contained in the data is retained by the first two principal components. This analysis enlightens about the positive or negative correlations among the many variables at play. For example, precipitation is highly positively correlated to latent heat fluxes, soil water content, relative humidity and cloud cover, whereas temperature is positively correlated to absorbed short-wave radiation and sensible heat fluxes, and negatively correlated to latent heat.

Minimum temperature does not significantly correlate with other variables, maybe owing to the reported underestimation of night cooling in CCLM [64]. Maximum temperature is more closely linked to sensible heat and surface evaporation.

4. Conclusions

This study offers a quantification of the regional effects on temperature and precipitation of large-scale idealized land cover changes in Europe with CCCLM. Changes in vegetation and surface moisture fluxes affect both average climate and occurrence of extreme temperatures. The temperature response to deforestation shows a clear latitudinal pattern, whose signal is stronger than the contrast of the local vs. regional impact. Forest clearance generally tends to cool annual mean temperature values at high latitudes, and warm at lower latitudes. In the entire domain, changes in latent heat fluxes dominate the regional climate response to forest clearance in summer, where both mean temperature values and hot temperature extremes are increased. Afforestation generally warms the local surface, but results are highly spatially heterogeneous at mid latitudes. Deforestation leads to increased summer temperature extremes, thereby underlining the importance of vegetation to keep a cooler climate in summer.



Possible extensions of this work include the possibility to quantify the impacts of both biophysical and biochemical effects, and constraint the range of the regional climate response in Europe to more realistic land use transitions and higher-resolution simulations. As a single model can have inherent limitations in terms of generalizability, future model inter-comparison studies can explore dependencies of results on individual models and configurations, and assess the sensitivity of the climate response to the spatial extent of the land cover change and across different resolutions. Further, more advanced experiments can investigate how explicit consideration of biochemical processes and future changes in climate can affect the results and associated uncertainty, in particular the dynamic response of the land cover through changes in phenology from climate feedbacks. For example, exchanges of CO_2 between vegetation and the atmosphere are sensitive to local climate conditions [65, 66], and future impacts of land-cover changes on regional climate can vary under a different future background climate [67].

As decisions are frequently taken at a subnational level by regional authorities, increasing the volume of information on regional and local climate impacts from land cover changes, and their effects of scale, can ultimately facilitate the design of more climate-oriented land use policies.

Acknowledgments

Authors acknowledge the support of the Norwegian Research Council (grants nr. 244074 and 254966). COSMO-CLM is the community model of the German regional climate research jointly further developed by the CLM-Community (www.clm-community.eu/). Simulations were performed on resources provided by UNINETT Sigma2—the National Infrastructure for High Performance Computing and Data Storage in Norway. We thank three anonymous reviewers for their useful inputs to the manuscript.

ORCID iDs

Francesco Cherubini  <https://orcid.org/0000-0002-7147-4292>

Merja H Tölle  <https://orcid.org/0000-0003-1958-2795>

References

- [1] Edelenbosch O Y 2016 *et al* Decomposing passenger transport futures comparing results of global integrated assessment models *Transport. Res. Part D: Transport Environ.* **55** 281–93
- [2] Popp A *et al* 2017 Land-use futures in the shared socio-economic pathways *Glob. Environ. Change* **42** 331–45

- [3] Popp A *et al* 2014 Land-use transition for bioenergy and climate stabilization: model comparison of drivers, impacts and interactions with other land use based mitigation options *Clim. Change* **123** 495–509
- [4] van Vuuren D P *et al* 2010 Bio-energy use and low stabilization scenarios *Energy J.* **31** 193–221
- [5] Clarke L and Jiang K 2014 Chapter 6: Assessing transformation pathways *Climate Change Mitigation—Contribution by Working Group III to the Fifth IPCC Assessment Report* (Geneva: IPCC) p 141
- [6] Mahmood R *et al* 2014 Land cover changes and their biogeophysical effects on climate *Int. J. Climatol.* **34** 929–53
- [7] Pielke Sr R A *et al* 2011 Land use/land cover changes and climate: modeling analysis and observational evidence *WIREs Clim. Change* **2** 828–50
- [8] Breil M and Schädler G 2017 Quantification of the uncertainties in soil and vegetation parameterizations for regional climate simulations in Europe *J. Hydrometeorol.* **18** 1535–48
- [9] Perugini L *et al* 2017 Biophysical effects on temperature and precipitation due to land cover change *Environ. Res. Lett.* **12** 053002
- [10] Georgescu M, Lobell D B and Field C B 2009 Potential impact of US biofuels on regional climate *Geophys. Res. Lett.* **36** L21806
- [11] Wang M *et al* 2017 On the long-term hydroclimatic sustainability of perennial bioenergy crop expansion over the United States *J. Clim.* **30** 2535–57
- [12] Davin E L and de Noblet-Ducoudré N 2010 Climatic impact of global-scale deforestation: radiative versus nonradiative processes *J. Clim.* **23** 97–112
- [13] Myklesby P M, Snyder P K and Twine T E 2017 Quantifying the trade-off between carbon sequestration and albedo in midlatitude and high-latitude North American forests *Geophys. Res. Lett.* **44** 2493–501
- [14] Bala G *et al* 2007 Combined climate and carbon-cycle effects of large-scale deforestation *Proc. Natl Acad. Sci.* **104** 6550–5
- [15] Bathiany S *et al* 2010 Combined biogeophysical and biogeochemical effects of large-scale forest cover changes in the MPI earth system model *Biogeosciences* **7** 1383–99
- [16] Li Y *et al* 2016 The role of spatial scale and background climate in the latitudinal temperature response to deforestation *Earth Syst. Dyn.* **7** 167–81
- [17] Li Y *et al* 2016 Potential and actual impacts of deforestation and afforestation on land surface temperature *J. Geophys. Res. Atmos.* **121** 14,372–86
- [18] Li Y *et al* 2015 Local cooling and warming effects of forests based on satellite observations *Nat. Commun.* **6** 6603
- [19] Lee X *et al* 2011 Observed increase in local cooling effect of deforestation at higher latitudes *Nature* **479** 384–7
- [20] Zhang M *et al* 2014 Response of surface air temperature to small-scale land clearing across latitudes *Environ. Res. Lett.* **9** 034002
- [21] Alkama R and Cescatti A 2016 Biophysical climate impacts of recent changes in global forest cover *Science* **351** 600–4
- [22] Findell K L *et al* 2017 The impact of anthropogenic land use and land cover change on regional climate extremes *Nat. Commun.* **8** 989
- [23] Seneviratne S I *et al* 2016 Allowable CO₂ emissions based on regional and impact-related climate targets *Nature* **529** 477–83
- [24] Leduc M, Matthews H D and de Elia R 2016 Regional estimates of the transient climate response to cumulative CO₂ emissions *Nat. Clim. Change* **6** 474–8
- [25] Orlovsky B and Seneviratne S I 2012 Global changes in extreme events: regional and seasonal dimension *Clim. Change* **110** 669–96
- [26] Tölle M H, Engler S and Panitz H-J 2017 Impact of abrupt land cover changes by tropical deforestation on Southeast Asian climate and agriculture *J. Clim.* **30** 2587–600
- [27] Betts R 2007 Implications of land ecosystem-atmosphere interactions for strategies for climate change adaptation and mitigation *Tellus B* **59** 602–15
- [28] Arora V K and Montenegro A 2011 Small temperature benefits provided by realistic afforestation efforts *Nat. Geosci.* **4** 514–8
- [29] Wramneby A, Smith B and Samuelsson P 2010 Hot spots of vegetation-climate feedbacks under future greenhouse forcing in Europe *J. Geophys. Res. Atmos.* **115** D21119
- [30] Seneviratne S I *et al* 2010 Investigating soil moisture–climate interactions in a changing climate: a review *Earth Sci. Rev.* **99** 125–61
- [31] Stéfanon M *et al* 2014 Soil moisture-temperature feedbacks at meso-scale during summer heat waves over western Europe *Clim. Dyn.* **42** 1309–24
- [32] Davin E L *et al* 2014 Preferential cooling of hot extremes from cropland albedo management *Proc. Natl Acad. Sci.* **111** 9757–61
- [33] Christidis N *et al* 2013 The role of land use change in the recent warming of daily extreme temperatures *Geophys. Res. Lett.* **40** 589–94
- [34] Bounoua L *et al* 2002 Effects of land cover conversion on surface climate *Clim. Change* **52** 29–64
- [35] Anav A *et al* 2010 Modelling the effects of land-cover changes on surface climate in the Mediterranean region *Clim. Res.* **41** 91–104
- [36] Strack J E *et al* 2008 Sensitivity of June near-surface temperatures and precipitation in the eastern United States to historical land cover changes since European settlement *Water Resour. Res.* **44** W11401
- [37] Lejeune Q *et al* 2018 Historical deforestation locally increased the intensity of hot days in northern mid-latitudes *Nat. Clim. Change* **8** 386–90
- [38] Prestele R *et al* 2017 Current challenges of implementing anthropogenic land-use and land-cover change in models contributing to climate change assessments *Earth Syst. Dyn.* **8** 369–86
- [39] Mahowald N M *et al* 2017 Are the impacts of land use on warming underestimated in climate policy? *Environ. Res. Lett.* **12** 094016
- [40] Davin E L, Maisonnave E and Seneviratne S I 2016 Is land surface processes representation a possible weak link in current regional climate models? *Environ. Res. Lett.* **11** 074027
- [41] Rechid D *et al* 2017 CORDEX flagship pilot study ‘LUCAS—land use and climate across scales’—a new initiative on coordinated regional land use change and climate experiments for Europe *Geophys. Res. Abstr.* **19** 13172
- [42] Rockel B, Will A and Hense A 2008 The regional climate model COSMO-CLM (CCLM) *Meteorol. Z.* **17** 347–8
- [43] Steppeler J *et al* 2003 Meso-gamma scale forecasts using the nonhydrostatic model LM *Meteorol. Atmos. Phys.* **82** 75–96
- [44] Wicker L J and Skamarock W C 2002 Time-splitting methods for elastic models using forward time schemes *Mon. Weather Rev.* **130** 2088–97
- [45] Arakawa A and Lamb V R 1981 A potential enstrophy and energy conserving scheme for the shallow-water equations *Mon. Weather Rev.* **109** 18–36
- [46] Schär C *et al* 2002 A new terrain-following vertical coordinate formulation for atmospheric prediction models *Mon. Weather Rev.* **130** 2459–80
- [47] Ritter B and Geleyn J F 1992 A comprehensive radiation scheme for numerical weather prediction models with potential applications in climate simulations *Mon. Weather Rev.* **120** 303–25
- [48] Schrodin R and Heise E 2002 The multi-layer version of the DWD soil model TERRA-LM *COSMO Tech. Rep. 2* (Offenbach: Deutscher Wetterdienst)
- [49] Doms G *et al* 2011 *A Description of the Nonhydrostatic Regional COSMO Model, Part II: Physical Parameterization* (Offenbach: DWD)
- [50] Davin E L *et al* 2011 COSMO-CLM2: a new version of the COSMO-CLM model coupled to the community land model *Clim. Dyn.* **37** 1889–907
- [51] Ament F and Simmer C 2006 Improved representation of land-surface heterogeneity in a non-hydrostatic numerical weather prediction model *Boundary Layer Meteorol.* **121** 153–74

- [52] Dee D P *et al* 2011 The ERA-Interim reanalysis: configuration and performance of the data assimilation system *Q. J. R. Meteorol. Soc.* **137** 553–97
- [53] Kotlarski S *et al* 2014 Regional climate modeling on European scales: a joint standard evaluation of the EURO-CORDEX RCM ensemble *Geosci. Model Dev.* **7** 1297–333
- [54] Tiedtke M 1989 A comprehensive mass flux scheme for cumulus parameterization in large-scale models *Mon. Weather Rev.* **117** 1779–800
- [55] Bartholomé E and Belward A S 2005 GLC2000: a new approach to global land cover mapping from Earth observation data *Int. J. Remote Sens.* **26** 1959–77
- [56] Tölle M H *et al* 2014 Increasing bioenergy production on arable land: Does the regional and local climate respond? Germany as a case study *J. Geophys. Res. Atmos.* **119** 2711–24
- [57] Sura P 2013 Stochastic models of climate extremes: theory and observations *Extremes in a Changing Climate: Detection, Analysis and Uncertainty* ed A AghaKouchak *et al* (Dordrecht: Springer) pp 181–222
- [58] Seneviratne S I *et al* 2012 Changes in climate extremes their impacts on the natural physical environment *Managing the Risks of Extreme Events and Disasters to Advance Climate Change Adaptation. A Special Report of Working Groups I and II of the Intergovernmental Panel on Climate Change (IPCC)* ed C B Field *et al* (Cambridge: Cambridge University Press) pp 109–230
- [59] Betts R A *et al* 2007 Biogeophysical effects of land use on climate: model simulations of radiative forcing and large-scale temperature change *Agric. Forest Meteorol.* **142** 216–33
- [60] Anderson R G *et al* 2010 Biophysical considerations in forestry for climate protection *Front. Ecol. Environ.* **9** 174–82
- [61] Cherubini F *et al* 2017 Spatial, seasonal, and topographical patterns of surface albedo in Norwegian forests and cropland *Int. J. Remote Sens.* **38** 4565–86
- [62] Jung M *et al* 2010 Recent decline in the global land evapotranspiration trend due to limited moisture supply *Nature* **467** 951
- [63] Tölle M H *et al* 2013 Water supply patterns over Germany under climate change conditions *Biogeosciences* **10** 2959–72
- [64] Vanden Broucke S *et al* 2015 New insights in the capability of climate models to simulate the impact of LUC based on temperature decomposition of paired site observations *J. Geophys. Res. Atmos.* **120** 5417–36
- [65] Sakaguchi K *et al* 2016 Influence of dynamic vegetation on carbon-nitrogen cycle feedback in the community land model (CLM4) *Environ. Res. Lett.* **11** 124029
- [66] Friend A D *et al* 2014 Carbon residence time dominates uncertainty in terrestrial vegetation responses to future climate and atmospheric CO₂ *Proc. Natl Acad. Sci. USA* **111** 3280–5
- [67] Pitman A J *et al* 2011 Importance of background climate in determining impact of land-cover change on regional climate *Nat. Clim. Change* **1** 472–5